CHARACTERIZATION OF THE SPATIAL UNIFORMITY OF THE TUZ GÖLÜ CALIBRATION TEST SITE

U. M. Leloğlu, S. Z. Gürbüz, H. Özen, S. Gürol

TÜBİTAK Space Technologies Research Institute, ODTÜ Campus, 06531 Ankara, Turkey
(leloglu, sevgi.gurbuz, hilal.ozen, selime.gurol)@uzay.tubitak.gov.tr

Commission VI, WG VI/4

KEY WORDS: Remote sensing, Radiometric Accuracy, Radiometry, Satellite Sensor, Calibration, Quality

ABSTRACT:

Based on absolute radiometric calibration studies conducted in 2008 and 2009 using ground measurements and satellite image data, Tuz Gölü, a salt lake in Central Turkey, was internationally acknowledged as an official CEOS cal/val test site. In particular, spatial uniformity and temporal stability are important qualities that are required of calibration test sites, as the homogeneity of the area effects site selection and the usability of test areas. In this study, the question of how to select a calibration test site in the lake that is the most homogenous and minimizes the number of ground sampling measurements is examined. The performance of Getis statistics in site selection is analyzed and it is observed that Getis statistics are not a good choice for uniformity analysis. Based on a power spectrum analysis of images, the error in continuous interpolation of in situ measurements was evaluated. However, further work is necessary to determine the actual error levels.

1. INTRODUCTION

Calibration and validation (cal/val) is an important process for ensuring the continuity, reliability, and therefore the widespread usability of satellite images from different sensors for earth observation applications. Typically, it is desired that test sites possess the following characteristics (Moraine and Budge, 2004; Teillet, et. al., 2007; Thome, 2002; Scott, et. al., 1996): 1) high reflectance, resulting in higher signal-to-noise ratio (SNR) and better overall accuracy; 2) spatial uniformity; 3) spectral uniformity; 4) temporal uniformity; 5) little or no vegetation; 6) sufficiently high altitude; 7) a Lambertian surface; 8) high probability of cloud free days; 9) sufficient distance from densely populated areas and industrial facilities; 10) sufficient distance from oceans or other large bodies of water; 11) minimal probability of precipitation; 12) sufficiently large area; 13) easy access; and 14) sufficient support of instrumentation. Considering the above criteria, therefore, generally deserts or dry salt lakes are preferred as radiometric calibration test sites.

The Committee on Earth Observation Satellites (CEOS) Working Group on Calibration and Validation (WGCV) Infrared and Visible Optical Sensors Group (IVOS) recently endorsed eight instrumented test sites as reference standards to serve calibration activities of land imagers, one of which includes Tuz Gölü, a salt lake in Central Turkey. In previous work (Gürol, et. al., 2008), homogeneity analysis of MODIS images taken in July and August of 2004-2007 were used to support the investigation of Tuz Gölü as a test site. In 2008, 2009 and 2010, field campaigns comprised of an international team of researchers were conducted. The most recent 2010 campaign included researchers from the National Aeronautics and Space Administration (NASA) and South Dakota State University in the USA, the National Physics Laboratory (NPL), UK, the French Aerospace Lab (ONERA), France, the Korean Aerospace Research Institute (KARI), S. Korea, the China Meteorological Administration (CMA), China, the Geo-Informatics and Space Technology Development Agency (GISTDA), Thailand, the Flemish Institute of Technological Research (VITO), Belgium, the Council for Scientific and Industrial Research (CSIR), South Africa, and the National Institute for Space Research (INPE), Brazil. The goal of these campaigns was to validate that indeed Tuz Gölü met the criteria for a radiometric calibration test site. Measurements for cross-comparison of instrumentation, site characterization and satellite radiometric calibration were conducted. Ground measurements of field spectroscopy, bidirectional reflectance distribution function (BRDF), meteorological and atmospheric conditions were taken. Additionally, radiometric calibration measurements for the imaging satellites UK-DMC, Beijing 1, Proba CHRIS, Deimos1, Avnir2, and Meris were accomplished.

While this data has shown the potential of Tuz Gölü as a vicarious radiometric calibration test site, the questions of how best to design such a field campaign in terms of site selection within the Tuz Gölü and optimal data collection strategy has yet to be addressed. This work attempts to lay the groundwork for a framework that would enable the selection of a site that is the most homogenous and minimizes the number of ground sampling measurements.

2. LANDNET SITE: TUZ GÖLÜ SALT LAKE

Tuz Gölü is a salt lake located in central Anatolia in Turkey (Fig. 1). Tuz Gölü has proven itself to satisfy the criteria defined by international Cal/Val community. Thus, it is one of the eight LANDNET Sites (CEOS Reference Sites).

The LANDNET Sites are a set of Land Equipped Sites (LES) endorsed by CEOS as standard reference sites for the post-launch calibration of space-based optical imaging sensors. During the CEOS IVOS-19 Meeting, held in Phoenix AZ, eight instrumented sites have been selected.

These instrumented sites are primarily used for field campaigns to obtain radiometric gain and these sites can serve as a focus

Figure 1. Location of the salt lake, Tuz Gölü (Gürol, et. al., 2008).

for international efforts, facilitating traceability and cross-comparison to evaluate biases of in-flight and future sensors in a harmonized manner (Cal/Val Portal).

3. RADIOMETRIC CALIBRATION

Ground-reference radiometric calibration techniques are based on predicting the radiance above the earth's atmosphere by taking ground measurements of the spectral radiance over a selected test site, and relating these ground measurements to the top of atmosphere radiance by taking into account the effects of the atmosphere (i.e., radiative transfer code), the spectral sensitivity of the imager, the bidirectional reflectance distribution function (BRDF) of the surface and other factors.

The spectral sensitivity of an imager is important as it affects the total radiance measured, as computed from the spectral radiance values given from the spectroradiometer. Define $g_i(f)$ as a function between frequencies F_1 and F_2 whose variation describes the sensitivity of the imager, and L_g as the spectral radiance measured by a spectroradiometer. Then, the total radiance L_T may be computed as

$$L_T = \int_{F_1}^{F_2} L_g g_i(f) df \,, \tag{1}$$

If unknown, the responsivity function is modeled as constant over the frequency range $[F_1, F_2]$.

The BRDF is defined as the ratio of reflected radiance exiting along zenith angle θ_o and azimuth angle ϕ_o to the incident irradiance impinging on the surface at zenith angle θ_i and azimuth angle ϕ_i:

$$BRDF(\theta_i, \phi_i, \theta_o, \phi_i) \equiv \frac{dL_r(\theta_o, \phi_o)}{dE_i(\theta_i, \phi_o)}, \tag{2}$$

where L_r is radiance, and E_i is irradiance. For a Lambertian surface, the apparent brightness of the surface is the same regardless of observation angle; thus, the BRDF is constant. In the framework of the field campaigns, the BRDF is also measured to minimize the errors from the Lambertian assumption.

Typically, during a campaign, radiances relative to a calibrated target are measured by a spectroradiometer, which can be converted to surface reflectances. Ground measurements are usually taken on the same day and time that an aerial or satellite image is taken. Besides, various atmospheric measurements are taken to determine the necessary parameters for the radiative transfer code.

There are many sources of error in the chain of calculations that are combined geometrically. One of the sources of error is the deviation from spatial uniformity. To reduce this error, the spectral radiance is measured at many points, making the ground calibration processes labor intensive and more costly. Thus, a key issue is how to determine what area of Tuz Gölü will minimize the required number of measurements, i.e. what region is the most homogenous.

4. GETIS STATISTICS

The Getis statistic (Getis and Ord, 1992) is defined as

$$G_i^*(d) = \frac{\sum_j w_{ij}(d) x_j - W_i^* \bar{x}}{s\left[W_i^*(n - W_i^*)/(n-1)\right]^{1/2}} \tag{3}$$

where $W_i^* = \sum_j w_{ij}(d)$, $\bar{x} = \frac{\sum_j x_j}{n}$, $s^2 = \frac{\sum_j x_j^2}{(n - (\bar{x})^2)}$,

$w_{ij}(d)$ is a spatial weight matrix, x_j is the digital number attributed to the pixel location index j, i is the target pixel location index and n is the total number of pixels. It was used by (Bannari, et. al., 2005) to evaluate the homogeneity of the Lunar Lake Playa, Nevada calibration test site. In our earlier studies, we have used the same method for Tuz Gölü and it generated sufficient results to analyze homogeneity; however, we would like to investigate the best possible function for this purpose.

Getis-like measures were originally proposed for analyzing geo-spatial data that can be distributed randomly in a plane. For remote sensing data, which is equally spaced in a rectangular grid, we can write the Getis formula in a slightly different form assuming a rectangular neighbourhood as usual:

$$G_d^*(i,j) = \frac{\sum_{k=i-d}^{i+d} \sum_{l=j-d}^{j+d} \left(x(k,l) - \bar{x}\right)}{s\left[W_i^*(n - W_i^*)/(n-1)\right]^{1/2}} \tag{4}$$

where *(i,j)* is the index of the target pixel and *d* is the diameter of the window. Basically, the nominator represents the absolute difference of the average within a window and the average of the full image. The parameter *s* is basically the standard deviation of the image and the factor

$\left[W_i*(n-W_i*)/(n-1)\right]^{1/2}$ is a constant. An important comment was made by J. K. Ord in (Ord, 2001) on the simpler form of the Getis formula, $G_d(i)$: "it is evident that the statistics are simply spatial moving averages, which are a form of kernel estimator defined over circular regions of radius *d* centered on the locations *v*. Similar definitions apply for other regional shapes."

Here, the definition of the "full image" is important, if we use areas outside the actual test area, then irrelevant information changes the statistics. If only the actual test area is used, then Getis statistics show us the positive and negative deviations within the test area, but cannot offer us a single parameter to measure the usefulness of this test area choice.

What we need is a parameter that shows the expected magnitude of the errors for a specific choice of the test site.

5. THE OPTIMALITY CRITERION

To find the best area and best sampling strategy, we need to define an error metric to minimize for a pixel to be calibrated. Since all operations are linear, we can change the order in the chain of operations from ground measurements to the top-of-the-atmosphere radiance values. As a result of recombination of the terms, we can reach the following expression for the actual measured radiance value at the imager

$$R = c\iint p(x,y)\, f(x,y)\, dx\, dy \tag{5}$$

where *p(x, y)* is the continuous point spread function (PSF, the mathematical function describing the imaging system's response to single point of light) of the imaging system (including the sampling of the CCD cell) back-projected on the earth, *f(x,y)* is the continuous function of radiance on the surface and *c* stands for all other operations, such as the radiative transfer code and BRDF, which are beyond the focus of this work.

The estimated radiance depends on the sampling points and the interpolation scheme. Let us assume sampling on a uniform grid. Then the sampling points are

$$\begin{aligned} x_i &= x_0 + i\tau \\ y_j &= y_0 + j\tau \end{aligned} \tag{6}$$

and

$$f[i,j] \equiv f(x_i, y_j) + n_{i,j}\,, \tag{7}$$

where τ is the sampling distance and $n_{i,j}$ is the measurement noise.

The simplest approach is to assume that the function *f(x,y)* is constant and to use the average of all measurements (sample mean) as the estimate of this constant function. In this case, Getis statistics can be used for selecting the best area by choosing *d* such that the window size matches the size of the area to be used. However, Getis statistics do not measure the variance within this window; they measure average deviation from the global mean.

A better approach, especially for very low resolution images, is to find the continuous interpolation of *f(x,y)* from samples (Oppenheim and Schafer, 1989) as

$$f_c(x,y) = \sum_i \sum_j f[i,j]\,\mathrm{sinc}(x - i\tau)\,\mathrm{sinc}(y - j\tau) \tag{8}$$

and to calculate

$$\hat{R} = c\iint p(x,y)\; f_c(x,y)\, dx\, dy \tag{9}$$

as the estimate of the measured radiance. Then, the error can be defined as the expected value of the squared difference

$$e = E\left\{\left(R - \hat{R}\right)^2\right\}. \tag{10}$$

Now, by combining (8) and (9), we obtain

$$\hat{R} = c\iint p(x,y) \sum_i \sum_j f[i,j]\,\mathrm{sinc}(x - i\tau)\,\mathrm{sinc}(y - j\tau)\, dx\, dy \tag{11}$$

which may be rearranged to find

$$\hat{R} = c\sum_i \sum_j f[i,j] \iint p(x,y)\,\mathrm{sinc}(x - i\tau)\,\mathrm{sinc}(y - j\tau)\, dx\, dy \tag{12}$$

If we assume that the function *f(x,y)* is smooth enough to be band limited with the frequency $f = \pm 1/2\tau$ cycles/pixel, then *R* can be written as an interpolation of samples from *f(x,y)* at the same points. The difference is found to be

$$R - \hat{R} = \sum_i \sum_j n_{i,j} \iint p(x,y)\,\mathrm{sinc}(x - i\tau)\,\mathrm{sinc}(y - j\tau)\, dx\, dy \tag{13}$$

Hence, the error is only a function of measurement noise if there is no aliasing. To understand the frequency content of *f(x,y)*, we first analyzed 32-m resolution Beijing-1 images of Tuz Gölü. The satellite images are actually samples of the function *f(x,y)*. Behaving like a low-pass filter, the PSF of the imagers does not allow considerable aliasing, hence it gives a good idea about the frequency content of the image above the Nyquist rate. For power spectrum estimation, we have chosen the 512 x 512 square area shown in Figure 2**Fehler! Verweisquelle konnte nicht gefunden werden.**. Table 1 shows basic statistics of this area. Unfortunately, we cannot directly tell how much of the variance is due to sensor noise and how much is due to the signal itself. Figure 3 depicts the power spectrum of all three bands in logarithmic scale. The $1/f^2$ curve is also drawn, which is observed in most natural images (Field, 1997). The lake image spectrum is consistent with the curve with the exceptions of a few small spikes, which suggest electromagnetic interference issues inside the camera electronics. If the rest of the function, which cannot be captured in the satellite image, follows the curve beyond the Nyquist rate, then we can say that there is even less energy in higher frequencies. However, the spectrum may have a peak at a certain scale due to geologic features.

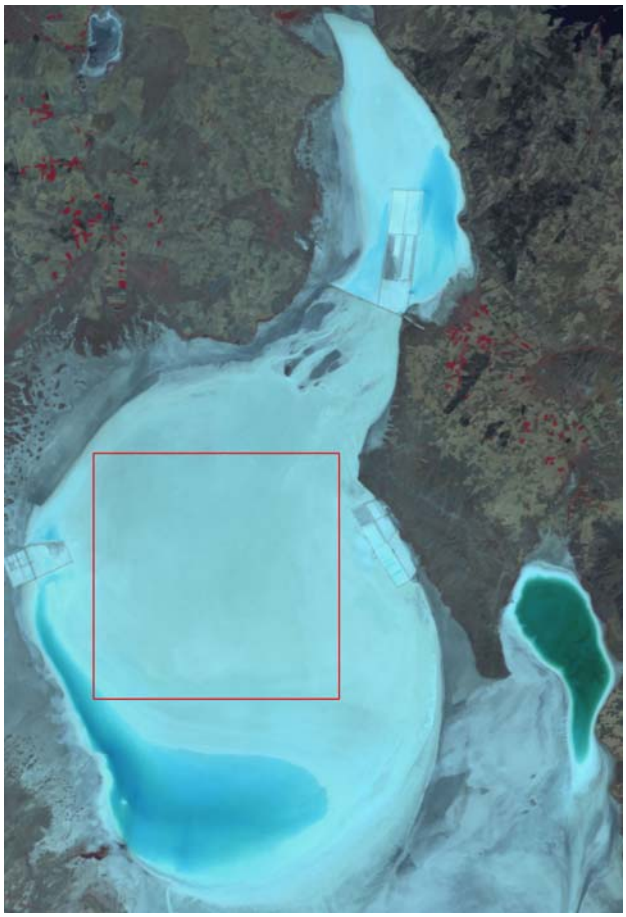

Figure 2. The 512x512 test area used for power spectrum estimation.

Band	Mean	Standard Dev.
Near IR	131.58	3.53
Red	205.81	4.83
Green	215.10	5.83

Table 1. First order statistics of test area.

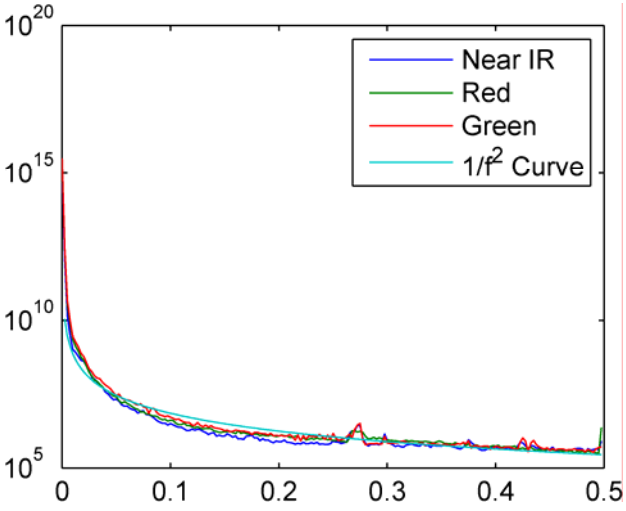

Figure 3. The power spectrum of the image of the test area.

6. CONCLUSIONS

To summarize, this work examines the utility of Getis statistics in determining the optimal calibration test site in terms of homogeneity and minimization of the number of ground sampling measurements required. Although Getis statistics may be applied for this purpose, Getis statistics do not measure the variance within the test window; rather, they measure average deviation from the mean. Thus, this work explores the error from integration of the inner product of the back-projected PSF and sinc-interpolated radiance. In future work, images at various resolutions, higher resolution images and in situ measurements will be analyzed to provide a quantitative performance comparison and determine the optimal sampling interval of data collection.

7. REFERENCES

Bannari, A., Omari, K., Teillet P.M., and Fedosejevs, G., 2005. Potential of Getis statistics to characterize the radiometric uniformity and stability of test sites used for the calibration of earth observation sensors. *IEEE Transactions on Geoscience and Remote Sensing*, 43(12), pp. 2918-2926.

Field, D. J., 1987. Relations between the statistics of natural images and the response properties of cortical cells. *J. Opt. Soc. Am. A,* Vol. 4, No. 12, pp. 2379-2394.

Getis, A., and Ord, J.K., 1992. The Analysis of Spatial Association by Use of Distance Statistics. *Geographical Analysis*, 24(3), pp. 189-206.

Gürol, S., Özen, H., Leloğlu, U. M., Tunalı, E., 2008. Tuz Gölü: New Absolute Radiometric Calibration Test Site, *Commission I, WG I/1, IRSPRS XXI Congress*, Beijing, China.

Morain S., and Budge M. A., 2004. *Post-Launch Calibration of Satellite Sensors,* ISPRS Book Series – Volume 2, pp.181-187.

Oppenheim, A.V., and Schafer, R.W., 1989. *Discrete-Time Signal Processing*, International Edition, Prentice Hall.

Ord, J. K., and Getis, A., 2001. Testing for Local Spatial Autocorrelation in the Presence of Global Autocorrelation. *Journal of Regional Science,* Vol. 41, pp. 411–432.

Scott, K. P., Thome, K., Brownlee, M. R., 1996. Evaluation of the Railroad Valley playa for use in vicarious calibration. *Proceedings of SPIE*, vol. 2818, pp. 158-166.

Teillet, P.M., Barsi, J.A., Chander, G., and Thome, K.J., 2007. Prime candidate earth targets for the post-launch radiometric calibration of space-based optical imaging instruments. *Proceedings of SPIE,* vol. 6677, 66770S.

Thome, K., 2002. Paper on the ISPRS Commission I Mid-Term Symposium in conjunction with Pecora 15/Land Satellite Information IV Conference "Ground look radiometric calibration approaches for remote sensing imagers in the solar reflective", Denver, CO USA.